The chaperone Hsp70 is a BH3 receptor activated by the pro-apoptotic Bim to stabilize anti-apoptotic clients

Received for publication, March 7, 2020, and in revised form, July 7, 2020 Published, Papers in Press, July 10, 2020, DOI 10.1074/jbc.RA120.013364

Zongwei Guo[1,‡], Ting Song[2,‡,*], Ziqian Wang[2], Donghai Lin[3], Keke Cao[1], Peng Liu[1], Yingang Feng[4], Xiaodong Zhang[2], Peiran Wang[2], Fangkui Yin[2], Jian Dai[2], Sheng Zhou[2], and Zhichao Zhang[2,*]

From the [1]School of Bioengineering, Dalian University of Technology, Dalian, Liaoning, China, the [2]State Key Laboratory of Fine Chemicals, Zhang Dayu School of Chemistry, Dalian University of Technology, Dalian, Liaoning, China, [3]The Key Laboratory for Chemical Biology of Fujian Province, MOE Key Laboratory of Spectrochemical Analysis and Instrumentation, College of Chemistry and Chemical Engineering, Xiamen University, Xiamen, Fujian, China, and the [4]Shandong Key Laboratory of Synthetic Biology, CAS Key Laboratory of Biofuels, Qingdao Institute of Bioenergy and Bioprocess Technology, Chinese Academy of Sciences, Qingdao, Shandong, China

Edited by Karen G. Fleming

The chaperone heat shock protein 70 (Hsp70) is crucial for avoiding protein misfolding under stress, but is also up-regulated in many kinds of cancers, where its ability to buffer cellular stress prevents apoptosis. Previous research has suggested Hsp70 interacts with pro-apoptotic Bcl-2 family proteins, including Bim and Bax. However, a definitive demonstration of this interaction awaits, and insights into the structural basis and molecular mechanism remain unclear. Earlier studies have identified a Bcl-2 homology 3 (BH3) domain present in Bcl-2 family members that engages receptors to stimulate apoptosis. We now show that Hsp70 physically interacts with pro-apoptotic multidomain and BH3-only proteins via a BH3 domain, thereby serving as a novel BH3 receptor, using *in vitro* fluorescent polarization (FP), isothermal titration calorimetry (ITC), and cell-based co-immunoprecipitation (co-IP) experiments, ^{1}H-^{15}N-transverse relaxation optimized spectroscopy (TROSY-HSQC), trypsin proteolysis, ATPase activity, and denatured rhodanese aggregation measurements further demonstrated that BimBH3 binds to a novel allosteric site in the nucleotide-binding domain (NBD) of Hsp70, by which Bim acts as a positive co-chaperone to promote the ATPase activity and chaperone functions. A dual role of Hsp70's anti-apoptotic function was revealed that when it keeps Bim in check to inhibit apoptosis, it simultaneously stabilizes oncogenic clients including AKT and Raf-1 with the aid of Bim. Two faces of Bim in cell fate regulation were revealed that in opposite to its well-established pro-apoptotic activator role, Bim could help the folding of oncogenic proteins.

Hsp70 is an ATP-dependent molecular chaperone that is abundantly expressed in most cancer cells to facilitate the maturation, activation, and stabilization of many oncogenic clients to buffer cellular stress (1–3). The chaperone function of Hsp70 is based on an allosteric mechanism, in which nucleotide-binding and conformation-specific co-chaperones regulate Hsp70-client protein interaction. As such, recruitment of Hsp70 by these co-chaperones would create a local pool of the chaperone to facilitate folding of clients (4, 5).

Besides, Hsp70 inhibits caspase-independent and caspase-dependent apoptosis by directly interacting with apoptosis-inducing factors, such as AIF and APAF-1, and inhibits caspase 3 and 9 activations (6, 7). However, as pivotal regulators of the mitochondrial apoptosis pathway, Bcl-2 family members have cross-talk with Hsp70 in a way that is not fully understood (8). Although a few previous reports have found Bim and Bax interactions with Hsp70 by co-IP and FRET (9–11), there is no solid evidence of the physical interactions between them. The biological consequence of these complexes is unknown.

The protein-protein interactions (PPIs) of the Bcl-2 family proteins dictate apoptosis, which is mediated by a Bcl-2 homology 3 (BH3) domain of the pro-apoptotic protein that inserts into a BH3 receptor groove on the surface of anti-apoptotic proteins (12). Recent pieces of evidence have revealed that BH3-only proteins could engage into BH3-receptor proteins besides the 16 well-known Bcl-2 family proteins (13–15), suggesting the presence of unknown BH3 receptors that have cross-talk with Bcl-2 members via a BH3 groove.

In this study, Bim was revealed that binds Hsp70 *in vitro* and in cells through the BH3 domain (a diagram of Bim sequence is shown in Fig. S1). Bim acts as a positive co-chaperone of Hsp70 because it increased ATPase activity and oncogenic chaperone functions of Hsp70 by stabilizing its ADP-binding conformation. In opposite to its classic role as an activator of intrinsic apoptosis, Bim was revealed that could help Hsp70 to stabilize oncogenic clients AKT and Raf-1.

Results and discussion

Characterization of the binding of Hsp70 to a panel of BH3 domains

We characterized the binding ability of Hsp70 proteins to BH3 domains of Bid, Bim, Noxa, Bax, and Bak by using *in vitro* biochemical assays and cell-based assays. Two Hsp70 inhibitors (VER-155008 (16) and MKT-077 (17)) were tested in parallel.

This article contains supporting information.

‡These authors contributed equally to this work.
*For correspondence: Prof. Ting Song, songting@dlut.edu.cn; Prof. Zhichao Zhang, zczhang@dlut.edu.cn.
Present address for Ting Song: State Key Laboratory of Fine Chemicals, Dalian University of Technology, Dalian, Liaoning, China.
Present address for Zhichao Zhang: State Key Laboratory of Fine Chemicals, Dalian University of Technology, Dalian, Liaoning, China.

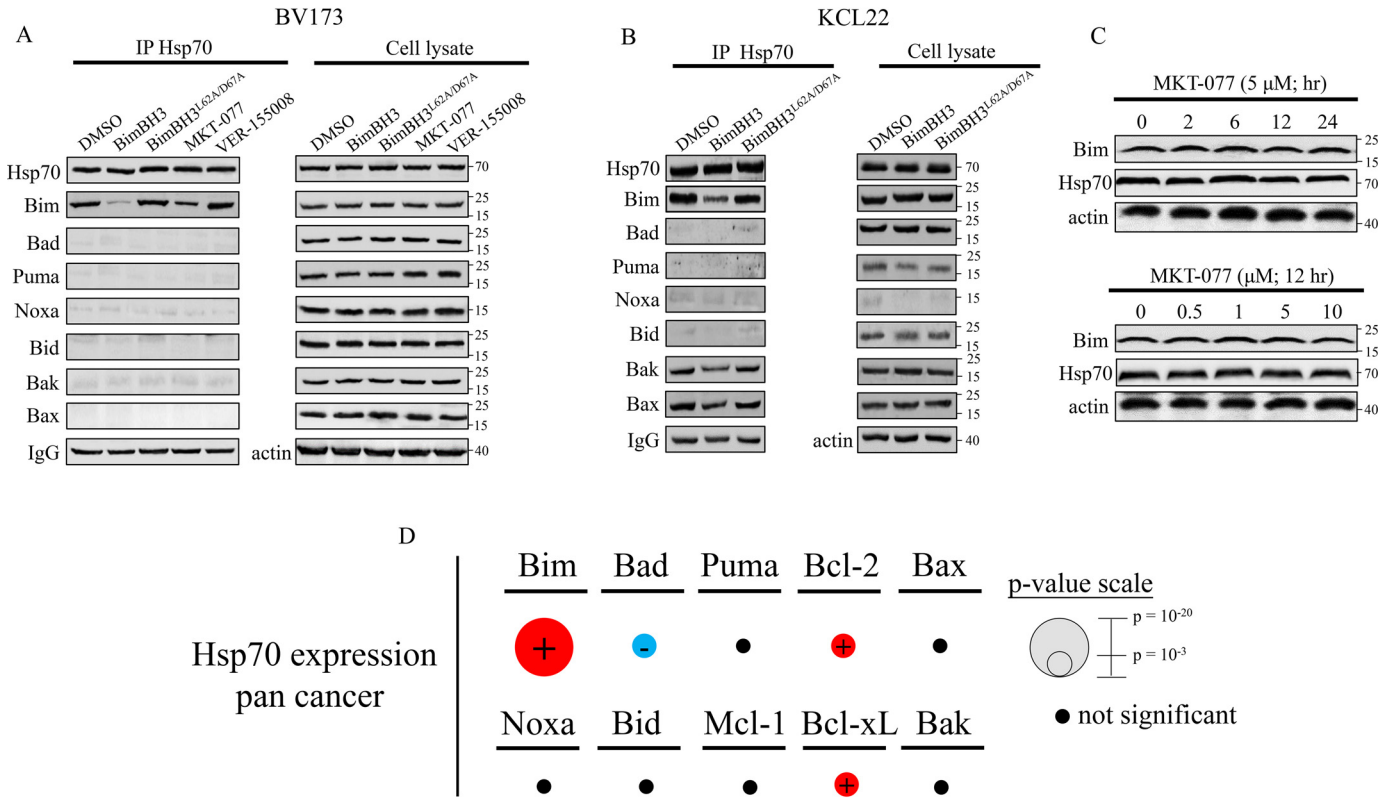

Figure 1. Profiling the interactions of Hsp70 with canonical pro-apoptotic and BH3-only Bcl-2 family proteins. Hsp70 was immunoprecipitated from BV173 (*A*) and KCL22 (*B*) cells, respectively, upon treatment with 5 μM BimBH3 peptide, 5 μM MKT-077, or 10 μM VER-155008 for 12 h, and immunoprecipitates were subjected to immunoblotting analysis for Bim, Bad, Puma, Noxa, Bid, Bak, and Bax proteins. *C,* BV-173 cells were treated with MKT-077 at 5 μM for 2, 6, 12, or 24 h (*top panel*), or with MKT-077 at 0.5, 1, 5, or 10 μM for 12 h (*bottom panel*), and the amounts of Bim was analyzed by immunoblotting. Data shown are representative of three independent experiments. *D,* CCLE database of all human cancers was probed for significant associations between the gene expression levels of Bim, Bad, Puma, Bcl-2, Bax, Noxa, Bid, Mcl-1, Bcl-xL, and Bak with Hsp70 from a sample of 837. Association strength is proportional to -log(*p* value), reflected in the radii of the *circles*. *Black circles* indicate nonsignificant association (*p* value cutoff = 0.02).

First, the specific binding effects of these BH3 peptides on apo-Hsp70 (nucleotide-free Hsp70) were evaluated through FP. As shown in Fig. S2, BH3 peptides derived from Bid, Bim, Noxa, Bax, and Bak exhibited direct binding affinities (K_d = 1.3-1.5 μM) to apo-Hsp70. MKT-077 could effectively compete the binding of BimBH3 to Hsp70 (IC_{50} = 3.2 μM), whereas VER-155008 failed to dissociate the BimBH3/Hsp70 complex (IC_{50} >100 μM). When mutating conserved BimBH3 resides Leu-62 and Asp-67 to alanine, it reduced the binding of BimBH3 to Hsp70 below detectable levels in our assay (K_d > 100 μM). FP results illustrated that the direct interactions of Bcl-2 family proteins with Hsp70 might be mediated by the BH3 domains, where MKT-077 but not VER-155008 might also occupy.

Next, we explored whether Hsp70 could bind Bcl-2 members through the BH3 domain in cells. Co-IP experiments were performed in BV173 and KCL22 cells to detect multidomain pro-apoptotic members and BH3-only pro-apoptotic members complexed with Hsp70. As shown in Fig. 1, *A* and *B*, the binding profiles of Hsp70 were found to be different in the two cell lines. Only Bim was observed at certain levels in complex with Hsp70 in both cell lines, whereas Bax and Bak were found to form heterodimers with Hsp70 only in KCL22 cells, suggesting the cell context-dependent Hsp70 complex with Bcl-2 proteins. No interactions were found between other BH3-only proteins (Bad, Puma, Noxa, and Bid) with Hsp70 in either of BV173 and KCL22. We further expanded the cell lines to His-23 and Lys-562, and continuously observed Bim interactions with Hsp70, whereas interactions with other BH3-only proteins were not found. Additionally, we detected some Hsp70/Bak complex but little Hsp70/Bax complex in Lys-562 and His-23 (Fig. S3). Then, we performed competitive experiments. As shown in Fig. 1, *A* and *B*, BimBH3 peptide efficiently disrupted the Hsp70/Bim interaction, indicating that Bim interacts with Hsp70 via BH3 domain in cells. The control $BimBH3^{L62A/D67A}$ peptide was ineffective. In addition, the Hsp70/Bim complex was potently disrupted by MKT-077, whereas weak to no disruption was found for VER-155008 (Fig. 1*A*), which is consistent with the *in vitro* binding profile.

Of note, the level of Bim remained constant for 2–24 h after it was released by 5 μM MKT-077, and it did not show any dose-dependent change with exposure to up to 10 μM compound (Fig. 1*C*). Hsp70-interacting protein can be divided into two groups: clients and co-chaperones. When the ATPase activity of Hsp70 is inhibited by inhibitors, for example, MKT-077, the client protein level would decrease (18). The unchanged Bim level after MKT-077 treatment indicated that Bim is likely to be a co-chaperone of Hsp70 rather than a client. Additionally, BimBH3 peptide binds to Hsp70 at higher binding affinity (K_d values at the submicromolar range) than the affinities of the reported client proteins (typically low to mid-

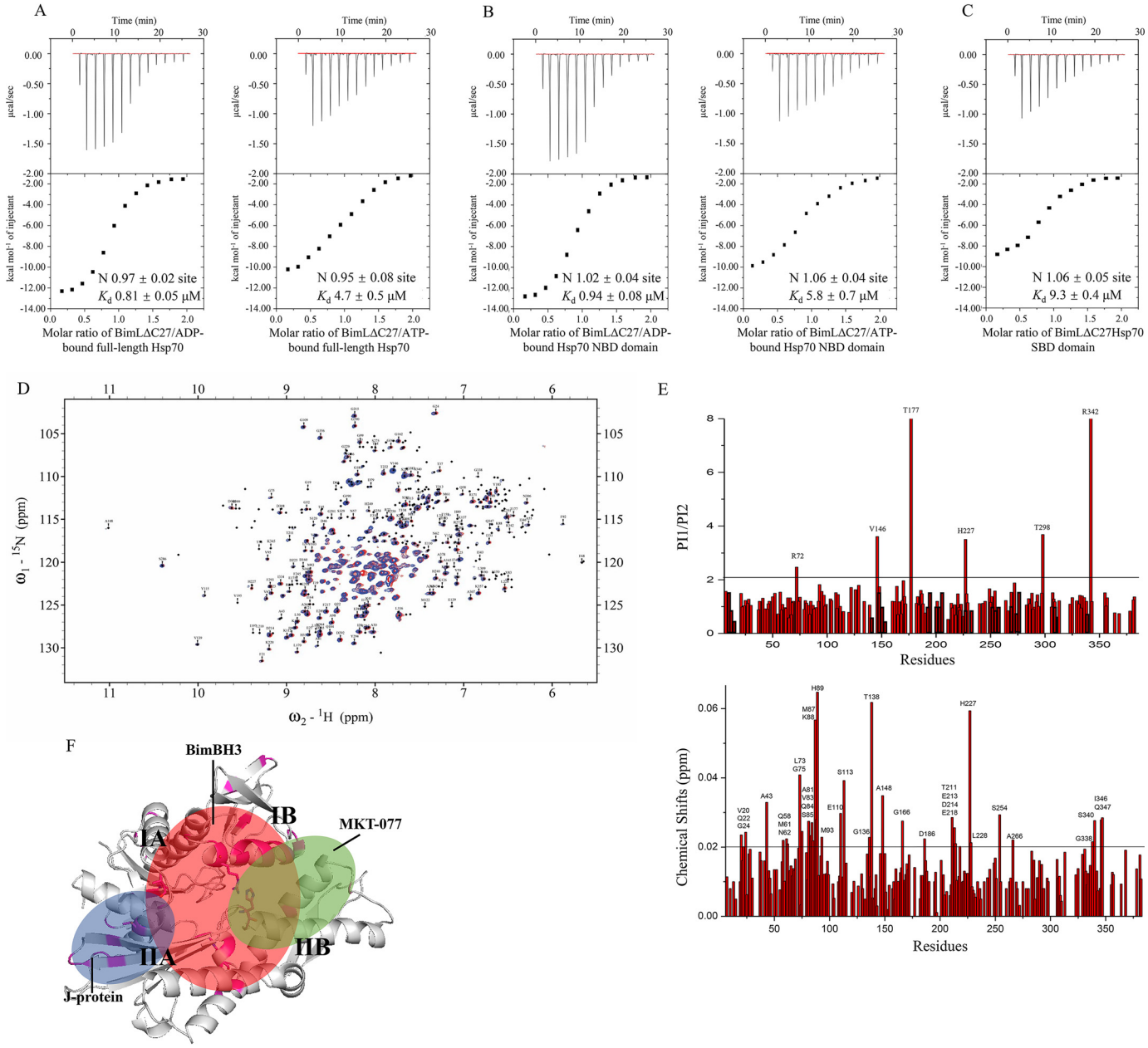

Figure 2. The binding site and conformational change effect of Bim in Hsp70 as determined by ITC, ^{1}H-^{15}N-TROSY NMR spectrum, and limited trypsin proteolysis. *A–C*, calorimetric isothermal titration measurement of the interaction of BimLΔC27 with ADP or ATP-bound full-length Hsp70 (*A*), ADP or ATP-bound Hsp70 NBD (*B*), and Hsp70 SBD (*C*). *Top*, raw data plot of heat flow against time for the titration of BimLΔC27 (300 μM) into Hsp70 (30 μM). *Bottom*, the respective integrated binding heat. The binding site N and K_d values were deduced from one-site curve fitting. The ITC data were shown as representative of three independent experiments. *D*, ^{1}H-^{15}N-TROSY-HSQC NMR spectra of ^{15}N-labeled Hsc70 NBD without (*red*) or with the addition of BimBH3 peptide (*blue*) in a ratio of 1:3. *E*, *top panel*: the peak intensity changes of Hsc70 NBD upon BimBH3 addition. *PI1* and *PI2* indicate peak intensity in the spectrum of apo-Hsc70 NBD and Hsc70 NBD/BimBH3 complexes, respectively. *Bottom panel*, the chemical shift perturbation of Hsp70 NBD upon BimBH3 addition. The chemical shift perturbations of cross-peaks are calculated as $[(\Delta H)^2 + (0.2\Delta N)^2]^{1/2}$, where ΔH represents the chemical shift change of the amide proton, and ΔN represents the chemical shift change of the amide nitrogen of an amino acid residue. Arbitrary thresholds value = mean value ± S.D. (0.02 ppm). *F*, labeling of the residues with significant chemical shift changes (*pink*) on Hsc70 NBD (Protein Data Base code 4H5T). *Green* and *blue circles* show the binding site of MKT-077 and J domain, respectively, as previously reported. *G*, limited trypsin proteolysis of apo-Hsp70, ATP, or ADP saturated Hsp70 upon addition of J domain and BimBH3 peptide. *Bands 1* and *2* were quantified in an ImageJ densitometer, and the ratio of these bands is shown in the *bottom panel*. Data are the mean ± S.D. ($n = 3$). The levels of significance were evaluated by two-tailed *t* test (**, $p < 0.01$).

micromolar) (19), which also indicated that Bim might be a co-chaperone of Hsp70 proteins rather than a client.

To explore the biological relevance of Bcl-2 family proteins with Hsp70 from a bioinformatics perspective, we examined publically available the CCLE database for gene expression data and determined association of Bcl-2 family protein expression with Hsp70 expression. Associations were examined in the pan-cancer (n = 837 across 16 cancers) (Table S1). As shown in Fig. 1*D* and Fig. S4, there is a significant correlation between Bim and Hsp70 expression ($r = 0.36$, $p = 10^{-20}$, 95% confidence interval of (0.31, 0.41)) (20). Compared with Bim, there were nonsignificant positive associations between other pro-apop-

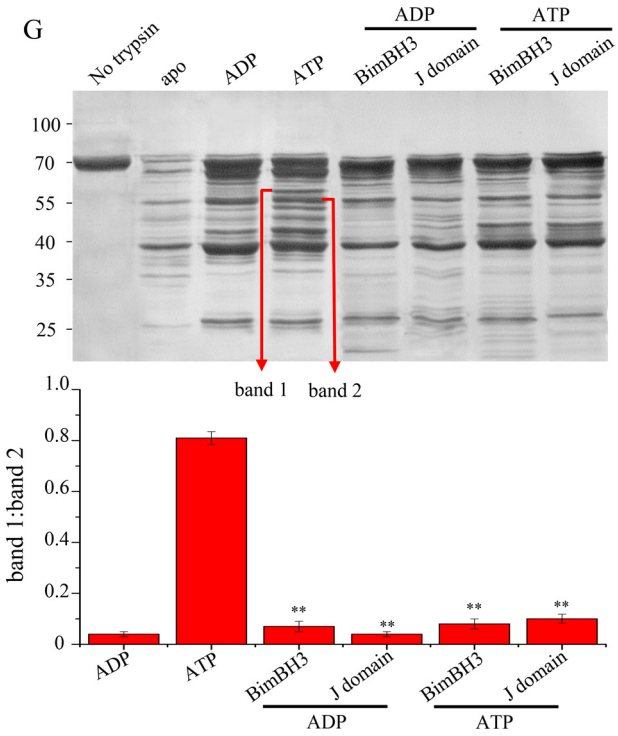

Figure 2. *—continued*

totic BH3-only and multidomain Bcl-2 family members with Hsp70.

The bioinformatics analysis highlights a related biological function between Hsp70 and Bim. Thus, we focus on Hsp70/Bim complex in the following study.

Localization of the interaction site of BimBH3 on Hsp70

To identify the interaction site for Bim on Hsp70, we expressed the recombination NBD (residues 1-383) and SBD (residues 397-506) of Hsp70, and analyzed the interaction of Bim with different nucleotide-bound states of Hsp70 by isothermal titration calorimeter (ITC). As shown in Fig. 2*A*, BimLΔC27 had a 6-fold higher binding affinity for ADP-bound full-length Hsp70 (K_d = 0.89 μM) (Fig. 2*A*, *left panel*) relative to ATP-bound Hsp70 (K_d = 5.3 μM) (Fig. 2*A*, *right panel*). Furthermore, we measured that BimLΔC27 exhibited essentially similar binding preference and affinity for ADP-bound Hsp70 NBD domain (K_d = 1.0 μM) relative to ATP-bound Hsp70 NBD (K_d = 6.4 μM) (Fig. 2*B*, *left* and *right panels*), whereas the interactions of the SBD domain appeared to be significantly weaker (K_d = 10.2 μM) (Fig. 2*C*). Although BimBH3 binds both NBD and SBD, no second binding event was apparent in the ITC curve of BimB3 to full-length Hsp70, suggesting that a close contact of NBD and SBD in full-length Hsp70 might form one binding unit for Bim, as similar as previously found in the Hsp70/Hsp40 complex (21). The significantly higher binding affinity of Bim to NBD than SBD showed that BimBH3 mainly interacts with Hsp70 NBD in an ADP-bound state and complements SBD by weak interactions.

To test whether BimBH3 resembles that full-length Bim, we assayed the binding affinity of BimBH3. As shown in Fig. S5, BimBH3 interacted with ADP-bound full-length Hsp70 (K_d = 0.81 μM), ADP-bound Hsp70 NBD (K_d = 0.94 μM), and Hsp70 SBD domain (K_d = 9.3 μM) as similar as BimLΔC27 did. Thus, it can be concluded that Bim interacts with the Hsp70 NBD domain via the BH3 domain.

Consequently, we performed ^{1}H-^{15}N-transverse relaxation optimized spectroscopy (TROSY) NMR experiments to explore the binding site of Bim on Hsp70 NBD domain. FP experiments showed that Hsc70 NBD binds BimBH3 as similar as Hsp70 NBD did (Fig. S6), which is consistent with the high similarity in Hsp70 and Hsc70. Because assignments of the backbone resonances of the Hsc70 NBD domain have been available in literature (22), we used a spectrum of ^{15}N-labeled Hsc70 NBD to localize the binding site (Fig. 2*D*). The resonance of 6 residues (Arg-72, Val-146, Thr-177, His-227, Thr-298, and Arg-342) showed a significant decrease in peak intensity (PI1/PI2 > 2), and 36 residues showed significant chemical shift changes (>0.02 ppm, Fig. 2*E*). All the residues showing significant peak intensity decrease (shown in *red sticks*) and more than 70% of the residues showing significant chemical changes (shown in *red*) were located in subdomains IA and IIA, surrounding a cleft opposite to the nucleotide-binding pocket, and therefore this cleft is indicated as the binding site of BimBH3 (Fig. 2*F*, *red circle*). To validate the binding site, we mutated His-227, one of the most disturbed residues in NMR experiment, and assayed the influence on Bim binding. By FP-based binding assay, we detected that compared with WT Hsp70 protein, the H227A mutant resulted in a 5-fold loss of binding affinity (Fig. S7), confirming the localization of the interaction site of Bim on Hsp70. Compared with MKT-077 and J-domain (Fig. 2*F*, binding sites were labeled in *green* and *blue circles*, respectively), BimBH3 binds into a site distinct from either of them. There is a region involved in both MKT-077 and BimBH3-binding areas, indicative of mutually exclusive binding. It is consistent with the competitive effect of MKT-077 against BimBH3 in FP and co-IP assays. The NMR results indicated that BimBH3 engaged in a site that is different from the previously known sites occupied by the J-domain or MKT-077. To test it, we performed FP-based binding between BimBH3 and Hsp70 in the presence or absence of the J-domain, and observed that the J-domain cannot influence the interaction between BimBH3 and Hsp70 (Fig. S7). The result confirmed that the binding site of Bim is different from J-domain.

Interacting proteins or small molecules that bind on the Hsp70 NBD domain often induce a conformational change between the ADP-like and ATP-like states. To evaluate whether Bim has such an effect, we performed trypsin treatment of human Hsp70. Consistent with previous reports (23), the addition of either ATP or ADP decelerated the proteolysis (Fig. 2*G*). Hsp70 saturated with ATP was primarily cleaved into three high-molecular mass bands, including prominent bands at ~58 kDa (band 1) and 55 kDa (band 2). Conversely, treatment with ADP strongly favored band 2. Addition of J domain, which stimulates ATP turnover in Hsp70, converted the ATP-like pattern into an ADP-like pattern, as shown by a significantly decreased ratio of band 1/band 2 than that in ATP-like state (**, $p < 0.01$, Fig. 2*G*, *bottom panel*). Addition of BimBH3 to Hsp70 significantly favored band 2, which is similar to the

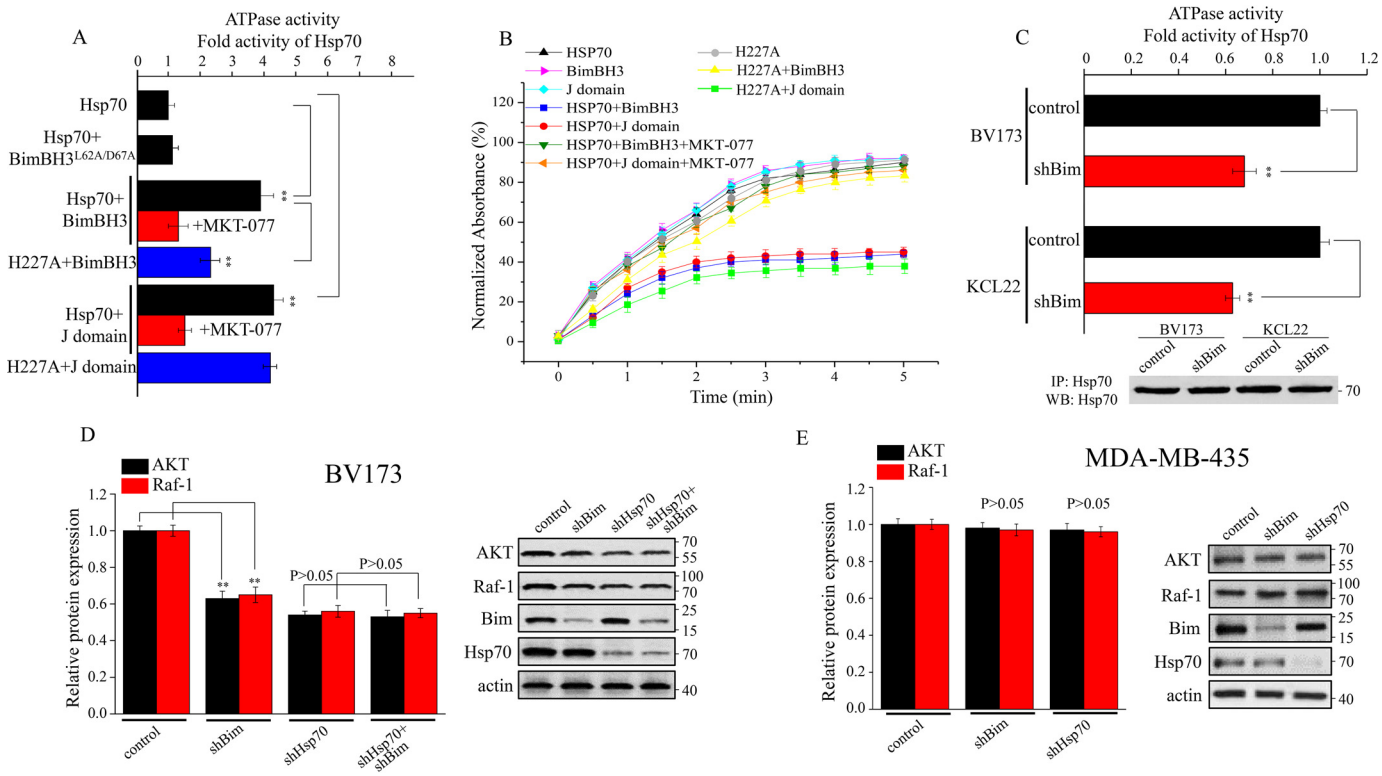

Figure 3. Effects of Bim on chaperone functions of Hsp70 *in vitro* and in cells. *A,* effects of BimBH3 (0.1 μM) or J domain (0.2 μM) on steady-state ATPase activity of Hsp70 and its H227A mutant (1 μM), respectively. MKT-077 was added at 50 μM. Data are the mean ± S.D. (n = 3). *B,* the aggregation of rhodanese was measured at 340 nm over 5 min. The measured optical densities were normalized to the zero reading for each well, and the increase in absorbance was plotted as a percentage of the total increase of rhodanese alone. Data are the mean ± S.D. (n = 3). *C,* ATPase activity of Hsp70 from BV173, Bim shRNA-transfected BV173, KCL22, and Bim shRNA-transfected KCL22. A same amount of Hsp70 from each cell sample is confirmed by immunoblotting. Data are the mean ± S.D. (n = 3). *D* and *E,* effects of shHsp70, shBim, or dual shHsp70 and shBim on the down-regulation of AKT and Raf-1 in BV173 (*D*) and MDA-MB-435 (*E*). Values in the column chart represent the relative protein levels of AKT and Raf-1 normalized to β-actin. Data are the mean ± S.D. (n = 3). The levels of significance were evaluated by two-tailed t test (**, $p < 0.01$, $P > 0.05$ shows no statistical significance).

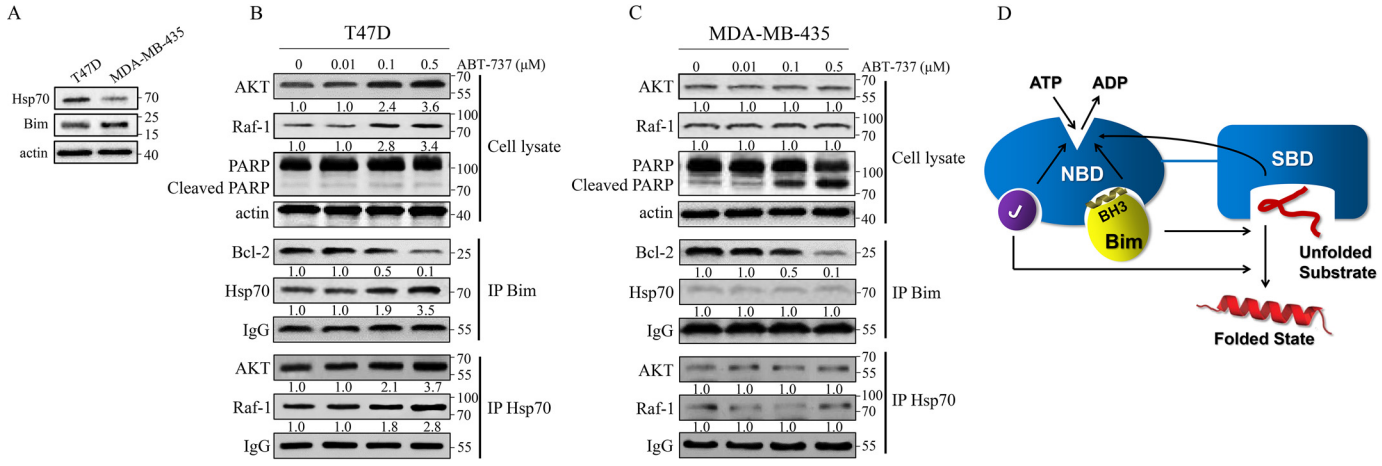

Figure 4. Effects of Hsp70 in ABT-737-induced apoptosis in T47D and MDA-MB-435 cells. *A,* expression levels of Hsp70 and Bim in T47D and MDA-MB-435 were determined by immunoblotting analysis. Data shown are representative of three independent experiments. T47D (*B*) and MDA-MB-435 (*C*) were treated with a gradient concentration of ABT-737 (0.01, 0.1, or 0.5 μM) for 24 h, after which levels of AKT, Raf-1, and cleaved PARP were determined by immunoblotting analysis. In parallel, Bim and Hsp70 were immunoprecipitated, respectively, from cells, and immunoprecipitates were subjected to immunoblotting analysis for corresponding proteins. Normalized densitometry measurements are indicated *below* the corresponding blots. Data shown are representative of three independent experiments. *D,* model for the mechanism of regulation of Hsp70 chaperone cycle by Bim.

influence of ADP and J domain. These results indicated that Bim binds preferentially to the ADP-bound state of Hsp70. The newly identified Bim-binding site is a novel allosteric site by which the ADP-bound conformation of Hsp70 could be stabilized. So far, the solid evidence of Bim binding with Hsp70 to act as an allosteric regulator has been shown, which prompted us to evaluate the effect of BimBH3 on ATPase and chaperone activities of Hsp70.

Identification of BH3-only protein Bim as a co-chaperone positively regulating the chaperone functions of Hsp70

We first evaluated the effect of Bim on Hsp70 ATPase. As shown in Fig. 3*A*, the combination of Hsp70 (1 μM) and BimBH3 (0.1 μM), which resembled the ratio of Bim-bound Hsp70 in total Hsp70 as determined by semi-quantification assay in cells (Fig. S8) resulted in a 3.8-fold increase of the rate of ATP consumption similarly to the addition of J domain (4.2-fold), and both of their stimulations of ATPase activity were blunted by MKT-077. The control BimBH3$^{L62A/D67A}$ peptide was ineffective. We also compared BimBH3 with σ^{32}, a model Hsp70's client. As shown in Fig. S9, *A* and *B*, BimBH3 could stimulate the ATPase activity of the Hsp70 NBD domain by 3.5-fold, which is similar to that of full-length Hsp70 (3.8-fold). In contrast, σ^{32} only stimulated full-length Hsp70 (2.2-fold) but not Hsp70 NBD. Compared with BimBH3 or J domain alone (3.6- and 4-fold, respectively), σ^{32} combination with BimBH3 or J domain stimulated ATP hydrolysis by 7.5- and 8.3-fold, respectively, suggesting that the combination could synergize to stimulate ATPase of Hsp70. However, the effect is abolished when using the Hsp70 NBD domain (Fig. S9*B*), suggesting that SBD is required for the synergistic effect.

Next, we measured the aggregation of denatured rhodanese by spectrophotometry to assess the effect of BimBH3 on Hsp70 chaperon activity. As shown in Fig. 3*B*, the addition of either BimBH3 or J domain in Hsp70 reduced rhodanese aggregation by 40–50%, indicative of the positive effect of BimBH3 on facilitating Hsp70 to bind and stabilize denatured rhodanese. MKT-077 inhibited these positive regulations of Hsp70 (Fig. 3*B*). Consistent with decreased Bim binding by the H227A mutant, the effect of BimBH3 on Hsp70 ATPase and aggregation of denatured rhodanese was significantly impaired by the mutant, whereas it did not influence the effect of J domain (Fig. 3, *A* and *B*). In agreement with BimBH3 peptide, we detected similar positive effects of BimLΔC27 on Hsp70 chaperon activity (Fig. S10). These results identified that Bim acts as a positive co-chaperone of the Hsp70 chaperone cycle.

To evaluate whether the *in vitro* biochemical assay represented the positive co-chaperone function of Bim in living cells, BV173 and KCL22 cells were transfected with Bim shRNA. As shown in Fig. S11, Bim shRNA transfection down-regulated the Bim protein level by about 90%, whereas Bim silence did not affect the level and complex state of Hsp70, Hsp40, and BAG3. Then, we immunoprecipitated Hsp70 from cell lysates of WT and Bim-silenced cells, respectively, and performed ATPase assays. As shown by Fig. 3*C*, Bim silence led to a down-regulation of the ATPase activity of Hsp70 by 30–40% in both BV173 and KCL22 cells, confirming the positive co-chaperone role of Bim in stimulating Hsp70 ATPase in cells.

Hsp70 is an important cancer chaperone that assists in the correct folding of oncogenic client proteins. The tumor addiction of Hsp70 may be enhanced by Bim because positive co-chaperones could up-regulate the level of clients and most reported so far are prosurvival proteins (24). We then evaluated regulation of the Hsp70/Bim complex on AKT and Raf-1, which are well-established clients of Hsp70 and are two important signaling proteins that control growth and anti-apoptosis of cancer cells (25). To test if Bim is involved in the control of these clients, we investigated whether Bim silence in BV173 affects levels of AKT and Raf-1. As shown in Fig. 3*D*, Bim silence caused a decreased level of AKT and Raf-1 by 38 and 35%, respectively, and Hsp70 silence caused a decreased level of AKT and Raf-1 by 44 and 42%, respectively. However, in cells with stable Hsp70 knockdown, Bim shRNA transient transfection had little effect on the levels of AKT and Raf-1 ($p > 0.05$, Fig. 3*D*). Therefore, the Hsp70/Bim complex is critical for stabilization of AKT and Raf-1. Similar effects of Hsp70 and Bim knockdown were detected in KCL22 and the breast cancer cell line T47D, demonstrating that these effects are widespread in multiple cancer types (Fig. S12). In line with it, when the shRNA experiments were performed in MDA-MB-435 that endogenously express a low level of Hsp70 protein, Hsp70 knockdown has no effect on the levels of AKT and Raf-1, and Bim knockdown paralleled the effect of Hsp70 (Fig. 3*E*). In summary, the Hsp70/Bim complex plays a critical role to facilitate the chaperone function of Hsp70 toward client proteins, which hinted that outcome of the Hsp70/Bim complex is to promote the oncogenic chaperone activity of Hsp70.

Furthermore, a dual role of Hsp70's anti-apoptotic function was illustrated in T47D and MDA-MB-435 cells following ABT-737 treatment that Hsp70 not only antagonizes Bim to protect cells from apoptosis, but also enhances the tumor chaperone's effect on stabilizing oncogenic clients with the help of the positive co-chaperone Bim.

Role of Hsp70/Bim complex in blocking cancer cells from apoptosis

ABT-737 is one of the most established small-molecule Bcl-2 inhibitors that induce intrinsic apoptosis by releasing pro-apoptotic Bim from Bcl-2 complexes. Its analog ABT-199 is the first FDA approved Bcl-2 inhibitor (26, 27). Although a previous report has found that mitochondria from T47D and MDA-MB-435 were similarly primed with Bim, only MDA-MB-435 cells exhibit the expected sensitivity to ABT-737 (28). Herein, we detected a much higher expression level of Hsp70 in T47D than in MDA-MB-435 cells (Fig. 4*A*). Then, we treated the two cell lines with a gradient concentration of ABT-737 and examined the composition of Bim and Hsp70 complexes. Protein levels of AKT, Raf-1, and PARP cleavage (a hallmark of apoptosis) were detected in parallel. As shown in Fig. 4*B*, for T47D, ABT-737 treatment induced a dose-dependent release of Bim from Bcl-2, which was not rebound to Bcl-xL and Mcl-1 (Fig. S13), whereas the Hsp70/Bim complex is increased, accompanied with increased AKT and Raf-1 binding with Hsp70 and up-regulation of the AKT and Raf-1 protein level. Even at 0.5 μM ABT-737 most of Bim were released from Bcl-2, and no PARP cleavage was detected. In addition, we assayed Hsp70 interactions with Bax and Bad, two other BH3-containing proteins that could be released from Bcl-2/Bcl-xL by ABT-737. Hsp70 showed very few interactions with Bax and Bad with little change after ABT-737 treatment (Fig. S13), confirming the cellular activity of the Hsp70/Bim complex in blocking apoptosis. In contrast, in MDA-MB-435 cells, very little Hsp70 was found in Bim complexes and no increase of Hsp70/Bim

complex was detected after ABT-737 treatment (Fig. 4*C*). Consistently, no increase of AKT and Raf-1 complex with Hsp70 and up-regulation of AKT and Raf-1 levels were detected. Meanwhile, PARP cleavage was detected as soon as Bcl-2/Bim was disrupted following 0.1 μM ABT-737 exposure, and the effects were further augmented at 0.5 μM ABT-737 (Fig. 4*C*). As reported by Letai and co-workers (28) and other groups, in ABT-737–resistant cells, activated AKT could induce Bax phosphorylation and switch Bax from promoting to inhibiting apoptosis, whereas activated ERK, a downstream effector of Raf-1, could promote Mcl-1 levels to confer ABT-737 resistance (29). Herein, we revealed that it is the high expression of Hsp70 that up-regulates AKT and Raf-1 with the help of Bim to antagonize ABT-737.

Tait *et al*. (30) previously reported that minority MOMP and DNA damage induced by nonlethal ABT-737 promotes tumorigenesis. Herein, we revealed that Bim released by nonlethal ABT-737 inhibits MOMP by facilitating stabilization of AKT/Raf-1. Given on the opposite role of Bim as a canonical BH3 activator to trigger MOMP by directly activating Bax/Bak, it is reasonable to suspect that the dual function of Bim might contribute to a balanced activation of Bax/Bak, which led to minority MOMP and DNA damage. Thus, further study will be directed to investigate how the paradoxical role of Bim promotes tumorigenesis.

To the best of our knowledge, our work is the first to describe that Bim binds in a new allosteric site of Hsp70 through the BH3 domain and then positively regulates its chaperone activity. Bim combination with the J domain has an addictive effect, and client binding can synergize with Bim or J domain to activate ATPase of Hsp70 (a model of the proposed reaction cycle was shown in Fig. 4*D*). It reminds us of a growing emergence of new partners of BH3-only protein, which endows BH3-only proteins with new roles on directly regulating the partners' activity and biological process beyond their canonical pro-apoptotic function (12, 13, 31). However, the new finding on Bim is unexpected. As the most predominant BH3-only protein that antagonizes all the anti-apoptosis Bcl-2-like proteins and acts as an activator of multidomain pro-apoptotic members, Bim conceals such an opposite role to help Hsp70 to stabilize oncogenic clients. There are some reports showing that cancer cells often express a significantly higher level of Bim than normal cells, which exhibits a prosurvival function (32). However, the molecular mechanism remains a mystery and people could not speculate why cancer takes the risk of overexpressing Bim. Our findings provide an unprecedented mechanism that being complexed with Hsp70 at least partly contributes to the Bim balancing between surviving and apoptosis.

Hsp70 protein was demonstrated to function as a BH3 receptor to capture Bcl-2 family members via the BH3 domain for the first time. Together with two previous reports of Hsp70/Bim and Hsp70/Bax complexes by co-IP (9, 10), Hsp70 can be listed into noncanonical Bcl-2-like proteins. Because the binding site of Bim is highly conserved among family members, such as Hsc70 (HSPA8), Hsp70 (HSPA1A), and GRP75 (HSPA9), as shown by sequence alignment (Fig. S14), nearly all Hsp70 family members are likely to act as BH3 receptors.

Taken together, the two-faced role of Bim in cell fate regulation and dual anti-apoptosis function of Hsp70 were revealed in this study. Moreover, the solid physical complex of Hsp70/Bim as well as the biological relevance between them as evidenced by bioinformatics analysis highlights the further exploration of the consequent biological events of Hsp70/Bim dimer in cell death and proliferation.

Materials and methods

Cell lines

Cell lines KCL22, BV-173, T47D, MDA-MB-435, K562, and H23 were purchased from American Type Culture Collection and used within 6 months from resuscitation. Cells were cultured in RPMI 1640 media (Thermo Scientific HyClone, Beijing, China) supplemented with 10% fetal bovine serum (Gibco BRL, Grand Island, NY) and 100 units/ml of penicillin and streptomycin at 37 °C and 5% CO_2.

Protein expression and purification

Constructs of hHsp70, hHsp70 NBD(1-383), and hHsc70 NBD(1-383) cDNA were subcloned into the pHis vector with a tobacco etch virus protease cleavage site for simple removal of the tag following protein production. The plasmids for full-length Hsp70, Hsp70 NBD, and Hsc70 NBD were prepared externally (Takara Bio Inc., Otsu, Japan). To construct Hsp70 mutant H227A, nucleotides corresponding to residue His-227 were substituted to create an alanine residue (Ala) with a site-directed mutagenesis kit (Clontech, Beijing, China). These proteins with an N-terminal His_6 tag were produced in *Escherichia coli* strain BL21 (DE3) containing the corresponding plasmid grown in LB medium at 37 °C to an optical density of 0.8 at 600 nm, and then induced by 0.5 mM isopropyl 1-thio-β-D-galactopyranoside at 37 °C for 5 h. For NMR studies, uniformly $^{2}H/^{15}N$-labeled protein samples were produced in D_2O minimal M9 medium, where $^{15}NH_4Cl$ were used as sole nitrogen sources. Cells were then lysed by sonication and the lysate was cleared by centrifugation at 9000 rpm for 30 min, and Hsp70 proteins were purified from the soluble fraction using nickel-nitrilotriacetic acid resin (Qiagen), following the manufacturer's instructions. The affinity tag was captured through reverse Ni^{2+} chromatography. The flow-through containing Hsp70 protein was further purified by Sephadex G-75 size exclusion chromatography (GE Healthcare). To make apo-Hsp70, the protein underwent extensive dialysis: day 1 was 25 mM HEPES, 100 mM NaCl, and 5 mM EDTA (pH 7.5), day 2, 25 mM HEPES, 100 mM NaCl, and 1 mM EDTA (pH 7.5), and day 3, 25 mM HEPES, 5 mM $MgCl_2$, and 10 mM KCl (pH 7.5).

For J domain expression, competent *E. coli* strain BL21 (DE3) was transformed with a plasmid that expresses bovine auxilin residues 810-910 as part of a glutathione *S*-transferase fusion protein. Transformed cells were grown in 1 liter of LB media to an OD of 0.4-0.7 at 37 °C, and expression of the fusion protein was induced by addition of isopropyl 1-thio-β-D-galactopyranoside to 1 mM. Cells were grown for 4 h at 25 °C, and harvested by centrifugation, and suspended in 40 ml of 50 mM Tris (pH 8.0), 1 mM DTT, 1 mM EDTA, 1 mM phenylmethylsulfonyl fluoride, and 5% glycerol. Cells were lysed by sonication

and the lysate was cleared by centrifugation at 9000 rpm for 30 min, and the supernatant was loaded onto 5 ml of GSH resin (GE Healthcare). The resin was washed with 50 mM Tris (pH 8.0), 1 mM DTT, 0.5 M NaCl, 1 mM EDTA, 1 mM phenylmethylsulfonyl fluoride, 0.1% Tween 20, 10 mM GSH, and 5% glycerol.

Isothermal titration calorimetry (ITC)

The Hsp70 protein interactions with BimBH3 peptide or BimLΔC27 were characterized using an isothermal titration microcalorimeter, ITC200 (GE Healthcare/MicroCal, South Burlington, VT) at 25 °C. The cell was loaded with 30 μM full-length Hsp70 or Hsp70 NBD in buffer A (5 mM $MgCl_2$, 25 mM KCl, 20 mM Tris-HCl, 3 mM ADP (pH 7.5)) and buffer B (5 mM $MgCl_2$, 25 mM KCl, 20 mM Tris-HCl, 3 mM ATP (pH 7.5)) respectively, by which ADP-bound full-length Hsp70, ATP-bound full-length Hsp70, ADP-bound Hsp70 NBD, or ATP-bound Hsp70 NBD were generated, and the injection syringe was loaded with 300 μM BH3 peptides or BimLΔC27. To assay BimBH3 peptide or BimLΔC27 binding with the SBD, the cell was loaded with 30 μM Hsp70 SBD in buffer C (5 mM $MgCl_2$, 25 mM KCl, 20 mM Tris-HCl (pH 7.5)). Typical titrations consisted of 12 injections of 3 μl. An additional set of injections was run in a separate experiment with buffer instead of the protein solution as a control. Before data analysis, the control values were subtracted from the main experimental data. The data were analyzed to fit a one-site model in MicroCal software.

NMR titrations

The experiments were performed at 26 °C on an 800-MHz Varian Inova NMR spectrometer equipped with a triple-resonance cold probe. Hsc70 NBD(1-383) samples (100 μM) in 5 mM $MgCl_2$, 25 mM KCl, 20 mM Tris-HCl, 10 mM ADP, 5 mM K_3PO_4, 0.005% sodium azide, and 10% (v/v) D_2O (pH 7.5) were used for the titrations, using 4 mM solutions of BimBH3 peptide in the above buffer.

Partial proteolysis

The partial proteolysis protocol was adapted from a previously described method (33). Briefly, Hsp70 (6 μM) in 40 mM HEPES buffer (20 mM NaCl, 8 mM $MgCl_2$, 20 mM KCl, and 0.3 mM EDTA (pH 8.0)) was incubated with either a buffer control, J domain (6 μM), or BimBH3 peptide (6 μM) when noted, with or without 1 mM nucleotide (ADP or ATP). Samples were incubated at room temperature for 30 min. The trypsin (EC 3.4.2.1.4; Sigma) was added to a final concentration of 0.9 μM, and the samples were incubated for another 30 min at room temperature. The reaction was then quenched with the addition of 25 μl of 3× SDS loading buffer (240 mM Tris, 6% (w/v) SDS, 30% (v/v) glycerol, 16% (v/v) β-mercaptoethanol, and 0.6 mg/ml of bromphenol blue (pH 6.8)) and heated to 95 °C for 3 min. Bands were separated by 12% SDS-PAGE and stained with Coomassie Blue.

ATPase activity

ATPase assays were carried out using Kinase-Lumi™ Plus Luminescent Kinase Assay Kit (Beyotime, China). Briefly, A master mix of full-length Hsp70 (final concentration 1 μM) was prepared in assay buffer (100 mM Tris-HCl, 20 mM KCl, and 6 mM $MgCl_2$ (pH 7.4)). An aliquot (50 μl) of this mixture and BimBH3 peptide (0.1 μM), J domain (0.2 μM), and σ^{32} (2 μM) alone or in combination in assay buffer were added to a 96-well–plate and incubated for 30 min at room temperature with or without MKT-077 (50 μM). The reaction was started by adding ATP (final concentration 40 μM). After reaction at 25 °C, 50-μl visualization reagents in the Luminescent Kinase Assay kit were added for 10 min. The enhanced chemiluminescence signal was determined with a SpectraMax M2e (Molecular Devices). To correct for nonenzymatic hydrolysis of ATP, the absorbance of a sample formed from an identically treated ATP buffer lacking the protein was subtracted. To detect HSP70 ATPase in BV-173, Bim shRNA-transfected BV173, KCL22, and Bim shRNA-transfected KCL22, HSP70 was co-immunoprecipitated from the above cell lysates, and then subjected to ATPase assay using Kinase-Lumi™ Plus Luminescent Kinase Assay Kit.

Rhodanese aggregation assay

The aggregation of denatured rhodanese was measured based largely on previously published procedures (34) with some modifications. Bovine liver rhodanese (30 mM; Sigma) was denatured in 6 M guanidine-HCl, 30 mM MOPS-KOH (pH 7.2), 2 mM DTT at room temperature for 30 min. The denatured rhodanese was diluted to a final concentration of 1.2 mM in buffer E (10 mM MOPS-KOH, pH 7.2), 50 mM KCl, 3 mM $MgCl_2$, 2 mM ATP, 2 mM DTT) in the presence or absence of 2 mM Hsp70, 0.4 mM J domain, 0.2 mM BimBH3 peptide, respectively, with or without 10 mM MKT-077. The aggregation of rhodanese was measured by the absorbance of light at 340 nm. The measured optical densities were normalized (to account for the addition of different proteins to the wells) to the zero reading for each well and the increase in absorbance plotted as a percentage of the total increase for rhodanese alone. More methods are provided under the supporting "Materials and methods."

Data availability statements

All the data supporting our conclusions are presented in this article.

Acknowledgments—Our NMR work was performed at the National Center for Protein Science Shanghai. We thank Bin Wu and Hongjuan Xue for the help at the facility. We thank Dr. Mahinur Akkaya (School of Bioengineering, Dalian University of Technology) for helping to modify the language.

Author contributions—Z. G., K. C., P. L., X. Z., and P. W. data curation; Z. G., T. S., Z. W., K. C., P. L., X. Z., P. W., and Z. Z. formal analysis; Z. G. investigation; Z. G., Z. W., D. L., K. C., P. L., Y. F., X. Z., and P. W. visualization; Z. G., P. L., X. Z., and P. W. methodology; T. S., P. W., and Z. Z. conceptualization; T. S., P. W., and Z. Z. supervision; T. S., P. W., and Z. Z. validation; T. S. writing-original draft; T. S., P. W., and Z. Z. project administration; Z. W.,

D. L., K. C., P. L., Y. F., X. Z., and P. W. software; Z. W., P. W., and Z. Z. funding acquisition; D. L., K. C., P. L., Y. F., X. Z., and P. W. resources; P. W. and Z. Z. writing-review and editing; Z. G. perform experiments; D. L. and Y. F. equipment (Nuclear Magnetic Resonance Spectrometer).

Funding and additional information—This work was supported by the National Natural Science Foundation of China Grants 81430083 and 81903462, China Postdoctoral Science Foundation Grant 2018M641694, and Fundamental Research Funds for the Central Universities Grant DUT20LK28.

Conflict of interest—The authors declare that they have no conflicts of interest with the contents of this article.

Abbreviations—The abbreviations used are: HSP, heat shock protein; IP, immunoprecipitation; PPI, protein-protein interactions; BH3, Bcl-2 homology 3; ITC, isothermal titration calorimeter; TROSY, 1H-15N-transverse relaxation optimized spectroscopy; FP, fluorescent polarization; shRNA, short hairpin RNA; NBD, nucleotide-binding domain; PARP, poly(ADP-ribose) polymerase; SBD, substrate-binding domain.

References

1. Murphy, M. E. (2013) The HSP70 family and cancer. *Carcinogenesis* **34,** 1181–1188 CrossRef Medline
2. Sherman, M. Y., and Gabai, V. L. (2015) Hsp70 in cancer: back to the future. *Oncogene* **34,** 4153–4161 CrossRef Medline
3. Wu, J. M., Liu, T. E., Rios, Z., Mei, Q. B., Lin, X. K., and Cao, S. S. (2017) Heat shock proteins and cancer. *Trends Pharmacol. Sci.* **38,** 226–256 CrossRef Medline
4. Taipale, M., Tucker, G., Peng, J., Krykbaeva, I., Lin, Z. Y., Larsen, B., Choi, H., Berger, B., Gingras, A. C., and Lindquist, S. (2014) A quantitative chaperone interaction network reveals the architecture of cellular protein homeostasis pathways. *Cell* **158,** 434–448 CrossRef Medline
5. Clerico, E. M., Tilitsky, J. M., Meng, W. L., and Gierasch, L. M. (2015) How Hsp70 molecular machines interact with their substrates to mediate diverse physiological functions. *J. Mol. Biol.* **427,** 1575–1588 CrossRef Medline
6. Creagh, E. M., Carmody, R. J., and Cotter, T. G. (2000) Heat shock protein 70 inhibits caspase-dependent and -independent apoptosis in Jurkat T cells. *Exp. Cell Res.* **257,** 58–66 CrossRef Medline
7. Beere, H. M. (2004) The stress of ding': the role of heat shock proteins in the regulation of apoptosis. *J. Cell Sci.* **117,** 2641–2651 CrossRef Medline
8. Rouf, R., and Kadry, S. (2019) Molecular chaperone HSP70 and key regulators of apoptosis: a review. *Curr. Mol. Med.* **19,** 315–325 CrossRef Medline
9. Ambrosini, G., Seelman, S. L., and Schwartz, G. K. (2009) Differentiation-related gene-1 decreases Bim stability by proteasome-mediated degradation. *Cancer Res.* **69,** 6115–6121 CrossRef Medline
10. Gotoh, T., Terada, K., Oyadomari, S., and Mori, M. (2004) Hsp70-DnaJ chaperone pair prevents nitric oxide- and CHOP-induced apoptosis by inhibiting translocation of Bax to mitochondria. *Cell Death Differ.* **11,** 390–402 CrossRef Medline
11. Park, S. H., Ko, W., Park, S. H., Lee, H. S., and Shin, I. (2020) Evaluation of the interaction between Bax and Hsp70 in cells by using a FRET system consisting of a fluorescent amino acid and YFP as a FRET pair. *ChemBiochem* **21,** 59–63 CrossRef Medline
12. Kelekar, A., and Thompson, C. B. (1998) Bcl-2-family proteins: the role of the BH3 domain in apoptosis. *Trends Cell Biol.* **8,** 324–330 CrossRef Medline
13. Szlyk, B., Braun, C. R., Ljubicic, S., Patton, E., Bird, G. H., Osundiji, M. A., Matschinsky, F. M., Walensky, L. D., and Danial, N. N. (2014) A phospho-BAD BH3 helix activates glucokinase by a mechanism distinct from that of allosteric activators. *Nat. Struct. Mol. Biol.* **21,** 36–42 CrossRef Medline
14. Rodriguez, D. A., Zamorano, S., Lisbona, F., Rojas-Rivera, D., Urra, H., Cubillos-Ruiz, J. R., Armisen, R., Henriquez, D. R., Cheng, E. H., Letek, M., Vaisar, T., Irrazabal, T., Gonzalez-Billault, C., Letai, A., Pimentel-Muinos, F. X., *et al.* (2012) BH3-only proteins are part of a regulatory network that control the sustained signalling of the unfolded protein response sensor IRE1α. *EMBO J.* **31,** 2322–2335 CrossRef Medline
15. Cooray, S., Bahar, M. W., Abrescia, N. G. A., Mcvey, C. E., Bartlett, N. W., Chen, R. A. J., Stuart, D. I., Grimes, J. M., and Smith, G. L. (2007) Functional and structural studies of the vaccinia virus virulence factor N1 reveal a Bcl-2-like anti-apoptotic protein. *J. Gen. Virol.* **88,** 1656–1666 CrossRef Medline
16. Wen, W., Liu, W. X., Shao, Y. F., and Chen, L. (2014) VER-155008, a small molecule inhibitor of HSP70 with potent anti-cancer activity on lung cancer cell lines. *Exp. Biol. Med.* **239,** 638–645 CrossRef Medline
17. Li, X. K., Srinivasan, S. R., Connarn, J., Ahmad, A., Young, Z. T., Kabza, A. M., Zuiderweg, E. R. P., Sun, D. X., and Gestwicki, J. E. (2013) Analogues of the allosteric heat shock protein 70 (Hsp70) inhibitor, MKT-077, as anti-cancer agents. *ACS Med. Chem. Lett.* **4,** 1042–1047 CrossRef
18. Budina-Kolomets, A., Balaburski, G. M., Bondar, A., Beeharry, N., Yen, T., and Murphy, M. E. (2014) Comparison of the activity of three different HSP70 inhibitors on apoptosis, cell cycle arrest, autophagy inhibition, and HSP90 inhibition. *Cancer Biol. Ther.* **15,** 194–199 CrossRef Medline
19. Cesa, L. C., Shao, H., Srinivasan, S. R., Tse, E., Jain, C., Zuiderweg, E. R. P., Southworth, D. R., Mapp, A. K., and Gestwicki, J. E. (2018) X-linked inhibitor of apoptosis protein (XIAP) is a client of heat shock protein 70 (Hsp70) and a biomarker of its inhibition. *J. Biol. Chem.* **293,** 2370–2380 CrossRef Medline
20. Cohen, J. (1988) *Statistical power analysis for the behavioral sciences*, 2nd Ed., L. Erlbaum Associates, Hillsdale, NJ
21. Weyer, F. A., Gumiero, A., Gesé, G. V., Lapouge, K., and Sinning, I. (2017) Structural insights into a unique Hsp70-Hsp40 interaction in the eukaryotic ribosome-associated complex. *Nat. Struct. Mol. Biol.* **24,** 144–151 CrossRef Medline
22. Zuiderweg, E. R. P., and Gestwicki, J. E. (2017) Backbone and methyl resonance assignments of the 42 kDa human Hsc70 nucleotide binding domain in the ADP state. *Biomol. NMR Assign.* **11,** 11–15 CrossRef Medline
23. Chang, L., Miyata, Y., Ung, P. M. U., Bertelsen, E. B., McQuade, T. J., Carlson, H. A., Zuiderweg, E. R. P., and Gestwicki, J. E. (2011) Chemical screens against a reconstituted multiprotein complex: myricetin blocks DnaJ regulation of DnaK through an allosteric mechanism. *Chem. Biol.* **18,** 210–221 CrossRef Medline
24. Calderwood, S. K. (2013) Molecular cochaperones: tumor growth and cancer treatment. *Scientifica (Cairo)* **2013,** 217513 CrossRef Medline
25. Pratt, W. B., Morishima, Y., Peng, H. M., and Osawa, Y. (2010) Proposal for a role of the Hsp90/Hsp70-based chaperone machinery in making triage decisions when proteins undergo oxidative and toxic damage. *Exp. Biol. Med.* **235,** 278–289 CrossRef Medline
26. Souers, A. J., Leverson, J. D., Boghaert, E. R., Ackler, S. L., Catron, N. D., Chen, J., Dayton, B. D., Ding, H., Enschede, S. H., Fairbrother, W. J., Huang, D. C. S., Hymowitz, S. G., Jin, S., Khaw, S. L., Kovar, P. J., *et al.* (2013) ABT-199, a potent and selective BCL-2 inhibitor, achieves antitumor activity while sparing platelets. *Nat. Med.* **19,** 202–208 CrossRef Medline
27. Deeks, E. D. (2016) Venetoclax: first global approval. *Drugs* **76,** 979–987 CrossRef Medline
28. Kale, J., Kutuk, O., Brito, G. C., Andrews, T. S., Leber, B., Letai, A., and Andrews, D. W. (2018) Phosphorylation switches Bax from promoting to inhibiting apoptosis thereby increasing drug resistance. *EMBO Rep.* **19,** e45235 CrossRef
29. Wang, B., Ni, Z. H., Dai, X. F., Qin, L. Y., Li, X. Z., Xu, L., Lian, J. Q., and He, F. T. (2014) The Bcl-2/xL inhibitor ABT-263 increases the stability of Mcl-1 mRNA and protein in hepatocellular carcinoma cells. *Mol. Cancer* **13,** 98 CrossRef
30. Ichim, G., Lopez, J., Ahmed, S. U., Muthalagu, N., Giampazolias, E., Delgado, M. E., Haller, M., Riley, J. S., Mason, S. M., Athineos, D., Parsons, M. J., de Kooij, B. V., Bouchier-Hayes, L., Chalmers, A. J., Rooswinkel, R. W., *et al.* (2015) Limited mitochondrial permeabilization causes DNA

damage and genomic instability in the absence of cell death. *Mol. Cell* **57,** 860–872 CrossRef Medline

31. Lomonosova, E., and Chinnadurai, G. (2008) BH3-only proteins in apoptosis and beyond: an overview. *Oncogene* **27,** S2–S19 CrossRef
32. Gogada, R., Yadav, N., Liu, J. W., Tang, S. H., Zhang, D. M., Schneider, A., Seshadri, A., Sun, L. M., Aldaz, C. M., Tang, D. G., and Chandra, D. (2013) Bim, a proapoptotic protein, up-regulated via transcription factor E2F1-dependent mechanism, functions as a prosurvival molecule in cancer. *J. Biol. Chem.* **288,** 368–381 CrossRef Medline
33. Rousaki, A., Miyata, Y., Jinwal, U. K., Dickey, C. A., Gestwicki, J. E., and Zuiderweg, E. R. P. (2011) Allosteric drugs: the interaction of antitumor compound MKT-077 with human Hsp70 chaperones. *J. Mol. Biol.* **411,** 614–632 CrossRef Medline
34. Ballinger, C. A., Connell, P., Wu, Y. X., Hu, Z. Y., Thompson, L. J., Yin, L. Y., and Patterson, C. (1999) Identification of CHIP, a novel tetratricopeptide repeat-containing protein that interacts with heat shock proteins and negatively regulates chaperone functions. *Mol. Cell Biol.* **19,** 4535–4545 CrossRef Medline